
PHASE
TRANSITIONS

On the Problem of the Existence of a Supercooled Liquid Phase of Cryovacuum Ethanol Condensates

A. Aldiyarov, A. Drobyshev*, E. Korshikov, V. Kurnosov, and D. Sokolov

Al-Farabi Kazakh National University, pr. al-Farabi 71, Almaty, 050040 Republic of Kazakhstan

* e-mail: Andrei.drobyshev@kaznu.kz

Received November 22, 2011

Abstract—Our previous IR-spectrometry and thermodesorption studies of thin films of cryovacuum ethanol condensates and comparison of these data with the data of some groups have allowed us to make several conclusions relative to temperature ranges of existence of low-temperature states of ethanol. Newly acquired experimental data indicate that the cryovacuum condensates of ethanol formed at considerably below the glass transition temperature $T_g \approx 98$ K pass through the state that can be characterized as a supercooled liquid phase in the course of subsequent thermally stimulated transformations. The temperature range of the solid–liquid transformation (97–100 K) agrees well with the data of researchers who studied the ethanol samples obtained by vitrifying from the liquid phase.

DOI: 10.1134/S1063783412070025

1. INTRODUCTION

One interesting fundamental problem of the physics of the solid state is the development of the theory of glass and vitrifying processes. Its solution will mean the intellectual breakthrough with far advanced heuristic and industrial consequences [1]. The characteristic objects of investigations in this aspect are the low-temperature forms of supercooled liquids and corresponding vitreous states. The modern state of the problem, new theories of relaxation processes, and experimental results are presented in review [2].

Hydrogen-bound systems, particularly water and ethanol, occupy the special place in the series of glass-forming substances under study. Despite the prolonged time of studying these materials and extended bibliography, the most important problems referring to dynamics of vitrification and glass transitions still remain unclear or disputable [3–6]. Not discussing the details, we note only the fact that there is still no the unique approach to classify the notion of the glass transition temperature for amorphous solid water (ASW) and its magnitude T_g . Our viewpoint for this matter is described in [7, 8].

In our opinion, the situation with vitrifying–melting in solid forms of ethanol seems to be no less problematic. The current state of the problem is described in detail in numerous publications [9–12], which allows us not to describe the problem in detail and immediately discuss our results. We previously studied the vapor-phase condensation of ethanol on cooled substrates at condensation temperatures $T = 16$ K and above. The pressure of the vapor phase was kept in the range from 10^{-2} to 10^{-4} Pa. Thus obtained thin films of solid ethanol are conventionally determined as cryo-

vacuum condensates. Our IR-spectrometry studies and the analysis of thermally stimulated relaxation processes in amorphous ethanol films [13–15] indicate the following. At above $T = 70$ – 80 K, the behavior of amorphous cryovacuum ethanol condensates is similar to the results of the studies where the samples of solid ethanol obtained from the liquid phase by ultrafast supercooling (quenching) were studied [9–12]. In the context of the accepted model of glass formation as a result of superfreezing of the liquid state, based on our data, we can assume that the low-temperature amorphous cryovacuum ethanol condensates, during their heating, also pass the stages glass–supercooled liquid–plastic crystal–monoclinic crystal. The problem arises if the intermediate state—supercooled liquid (SCL)—exists for vitreous samples of ethanol cryogenic condensates, the biography of which did not include the liquid phase as such. These investigations are an attempt to solve this problem.

2. RESULTS AND DISCUSSION

Our previous IR-spectrometry and thermodesorption studies of thin films of cryovacuum ethanol condensates [13–15] and comparison of these results with the data [12, 16] allowed us to make some assumptions relative to the existence ranges of the known low-temperature forms of ethanol. Figure 1 shows the comparison of the heating curve of a thin film of the ethanol cryogenic condensate [13] with the phase diagram of the monolithic ethanol sample obtained from the liquid phase by superfreezing [12].

Observation frequency $\nu = 3105$ cm^{-1} corresponds to the absorption half-width of the O–H bond of the

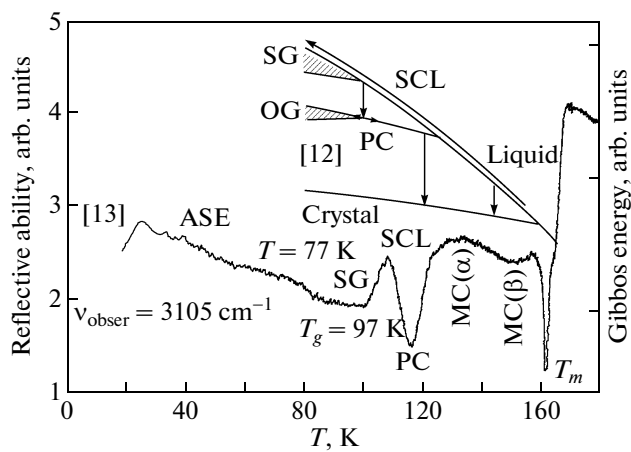


Fig. 1. Comparison of the heating curve of a thin film of the ethanol cryogenic condensate [13] with the phase diagram of the monolithic ethanol sample obtained from the liquid phase [12]. SG is the structural glass, SCL is the supercooled liquid, OG is the orientational glass, ASE is the amorphous solid ethanol, PC is the plastic crystal, MC(α) is the monoclinic crystal (α -phase), MC(β) is the monoclinic crystal (β -phase), and T_g is the glass transition temperature.

ethanol molecule, which is very sensitive to structural transformations in hydrogen-bound cryovacuum condensates, particularly in water and ethanol. Thus, the features of behavior of the IR-spectrometer signal at this frequency can be indicators of structural transformations. It is seen from the comparison of the phase diagram and heating curve that there is a clear correlation of temperatures corresponding to structural transformations in the diagram with the trend features of the heating curve, which correspond either to the shift

of valence vibrations of the O–H bond or to the variation in the absorption amplitude.

Based on these data, we measured the IR spectra of thin ethanol films formed at condensation temperature $T = 16$ K (amorphous state) and sequentially heated to $T = 112$ K (SCL or plastic crystal) and $T = 120$ K (monoclinic crystal). Dried ethanol of the 99.99% purity grade was used in the experiments. These data along with the heating curve are presented in Fig. 2. The upper curve reflects the character of the trend of the spectrometer signal during heating (the upper and right scale). The distinction of the IR spectra of the samples obtained at condensation temperature $T = 16$ K and heated to $T = 120$ K is caused by their different structural states, namely, amorphous and crystalline. As for curve 3, we assume that its character is caused by scattering of the high-frequency part of the spectrum by the sample, which is either the supercooled liquid or the plastic crystal.

A fragment of a longer-wavelength part of the spectrum presented in Fig. 3 shows the essential variations in the spectrum of the sample obtained upon heating to $T = 112$ K in more detail. They consist in a considerable broadening of absorption bands referred to combinations of stretching vibrations $\nu(\text{CCO})$ with rotational vibrations of methyl $\nu(\text{CH}_3)$ and methylene $\nu(\text{CH}_2)$ groups and deformational vibrations of $\delta(\text{OH})$ bond (the group of bands in a range of $1000\text{--}1250\text{ cm}^{-1}$). In addition, in spectrum 2, these bands are noticeably shifted towards lower frequencies. The band centered at frequency $\nu = 880\text{ cm}^{-1}$, which is identified as stretching vibrations of the CCO bond, is noticeably broadened and shifted into the red region. In addition, a fine structure in a form of spectral perturbations appears for this band. Based on the described features,

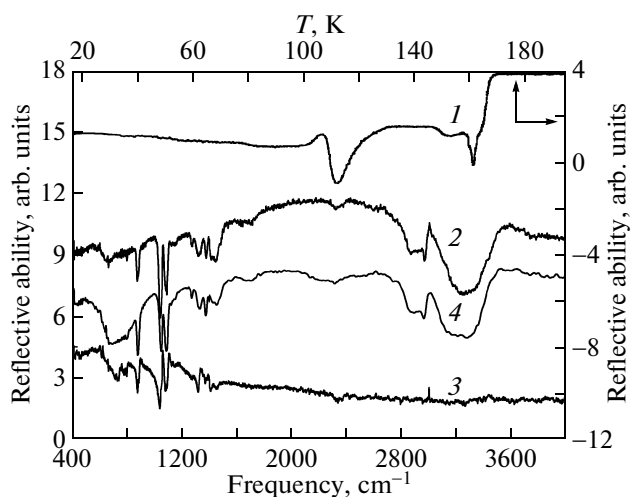


Fig. 2. Variation in the IR signal at fixed frequency $\nu = 3105\text{ cm}^{-1}$ (1) during heating and the IR spectra of the ethanol cryogenic condensate $0.75\text{ }\mu\text{m}$ thick (2) after condensation at $T = 16$ K, (3) after heating from $T = 16$ K to 112 K, and (4) after heating from $T = 16$ K to 120 K.

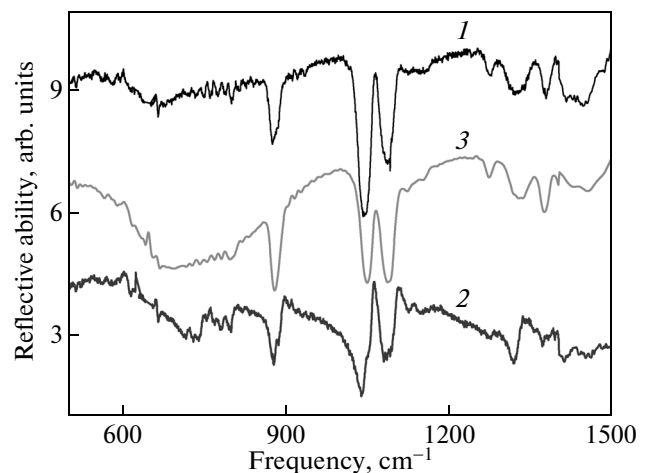


Fig. 3. IR spectra of the ethanol cryogenic condensate $0.75\text{ }\mu\text{m}$ thick. (1) After condensation at $T = 16$ K, (2) after heating from $T = 16$ K to 112 K, and (3) after heating from $T = 16$ K to 120 K.

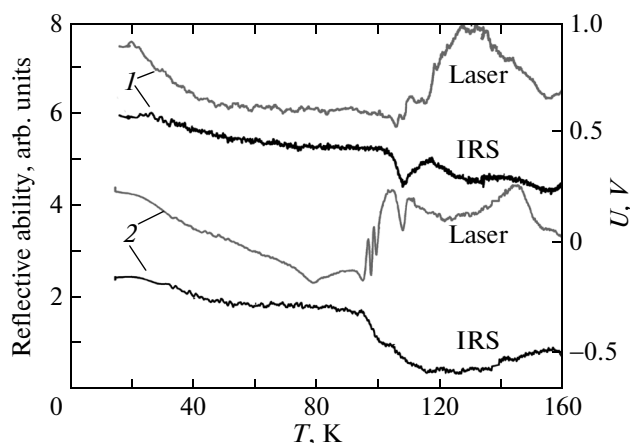


Fig. 4. Variation in signals of the IR spectrometer (IRS) at fixed frequency $\nu = 3105 \text{ cm}^{-1}$ and signals of the laser interferometer (Laser) with increasing the temperature. (1) The ethanol film is $3 \mu\text{m}$ thick and condensation temperature $T = 16 \text{ K}$; and (2) the ethanol film is $2.5 \mu\text{m}$ thick, the water film is $0.25 \mu\text{m}$ thick, and condensation temperature $T = 16 \text{ K}$.

we can conclude that a weaker intermolecular interaction and the appearance of additional degrees of freedom is characteristic of ethanol heated to $T = 112 \text{ K}$, for example, due to the appearance of additional degrees of freedom, for example, due to the unfrozen rotational subsystem of the plastic crystal or the supercooled liquid.

Based on the performed IR-spectrometry studies, we can conclude that the properties of the heated ethanol film in the temperature range from 96 to 116 K substantially differ from these at a lower temperature (glass) and at a higher temperature (crystal). However, based on the performed studies only, we cannot unambiguously affirm, what of two probable states, namely, supercooled liquid or the plastic crystal, is the cause of observed distinctions. In connection with this, we performed additional studies with the simultaneous use of the IR spectrometer and a laser interferometer (He–Ne), which we use to determine the refraction index, film thickness, and its formation rate. It was assumed that as ethanol passes the sequence of states amorphous–vitreous–liquid–crystalline, glass melting and formation of the supercooled liquid should be accompanied by the variation in the optical density of the medium and by the interference of the laser beam. These results are presented in Fig. 4.

It is seen from Fig. 4 that the data of thermograms correlate well with the assumed transformations in ethanol (Fig. 1). However, the variation in intensity of the signal of the laser interferometer in the temperature range of presumable SCL existence weakly manifests itself (pair of curves 1 in Fig. 4). This is apparently associated with the closeness of the values of refraction indices of the vitreous and liquid states. In connection with this, the variations were introduced into the

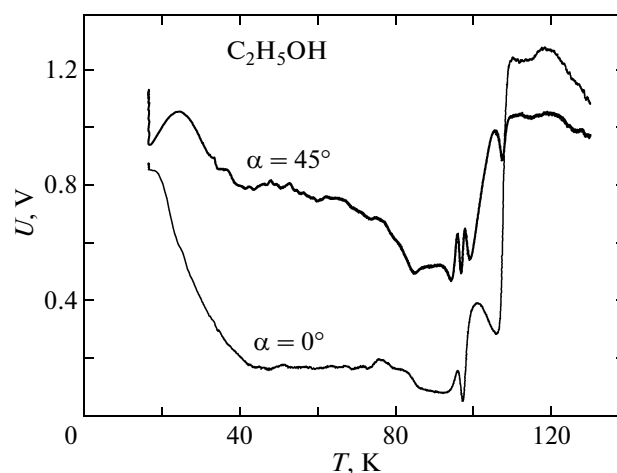


Fig. 5. Variation in signals of the laser interferometer at various observation angles with increasing the temperature. Condensation temperature $T = 16 \text{ K}$, the ethanol film is $2.5 \mu\text{m}$ thick, and the water film is $0.25 \mu\text{m}$ thick.

experimental procedure, the essence of which is in that a thin layer of water cryocondensate $0.25 \mu\text{m}$ thick was additionally deposited on the surface of the ethanol film $2.5 \mu\text{m}$ thick condensed at $T = 16 \text{ K}$. It was assumed that ice can dissolve in the quasi-liquid ethanol phase when this bilayer film passes through the SCL state of ethanol, which can cause the interference effect. The results of such experiment are presented in lower thermograms (pair of curves 2 in Fig. 4). The upper thermogram is the photomultiplier signal to the radiation of the He–Ne laser reflected from the sample, and the lower curve is the signal of the IR spectrometer at an observation frequency of 3115 cm^{-1} .

It is seen that the behavior of the upper thermogram can be unambiguously related to the characteristic temperatures of structural transformations in the ethanol film. For example, we previously [13] interpreted temperature $T = 78 \text{ K}$ as the transition temperature from the amorphous state ASW to state Glass similar to the glass obtained under supercooling of the liquid phase. Starting from $T = 94 \text{ K}$, according to the thermogram of the IR spectrometer, the transition of glass into the state of the supercooled liquid occurs. This process is accompanied by the clearly pronounced interference of the laser radiation, which occurs up to $T = 107 \text{ K}$. We assume that this fact is a direct consequence of melting the ethanol glass with the formation of the SCL, in which a thin film of solid water dissolves. This leads to an essential variation in the optical density of the medium interacting with the laser radiation.

Figure 5 represents the results of similar observations for various angles of incidence of the laser radiation. It is seen that these results agree well with the data of Fig. 4. The distinction between the upper and lower curves is the consequence of the difference of the opti-

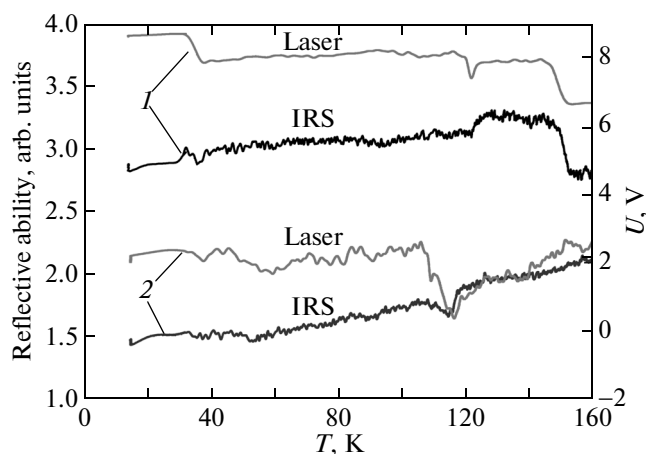


Fig. 6. Variation in signals of the IR spectrometer (IRS) at fixed frequency $\nu = 3115 \text{ cm}^{-1}$ and signals of the laser interferometer (Laser) with increasing the temperature. (1) The ethanol film is $2.5 \text{ }\mu\text{m}$ thick and condensation temperature $T = 130 \text{ K}$; and (2) the ethanol film is $2.5 \text{ }\mu\text{m}$ thick, condensation temperature of ethanol $T = 130 \text{ K}$, the water film is $0.25 \text{ }\mu\text{m}$ thick, and condensation temperature of water $T = 16 \text{ K}$.

cal path length of the laser radiation for observation angles of 0 and 45° .

According to our assumptions, when the ethanol sample condenses at a temperature higher than the glass transition temperature, no subsequent thermal variations should lead to the variations in signals of the IR spectrometer and laser interferometer corresponding to the glass–liquid transition. Figure 6 represents the experimental results that confirm this assumption. The upper thermograms (pair of curves 1) correspond to the experiment, during which the ethanol film $2.5 \text{ }\mu\text{m}$ thick condensed at $T = 130 \text{ K}$, i.e., above glass transition temperature $T = 97 \text{ K}$. After this, the sample was cooled to $T = 16 \text{ K}$ and slowly heated with the observation at a fixed frequency of the IR spectrometer ($\nu = 3115 \text{ cm}^{-1}$) and using the laser interferometer. Pair of curves 2 is the result of a similar experiment with the difference that a thin water layer $0.25 \text{ }\mu\text{m}$ thick was condensed on the film surface after cooling to $T = 16 \text{ K}$.

It is seen from the data presented in Fig. 6 that in both cases, the features in the behavior of thermograms near the glass transition temperature for ethanol $T = 97 \text{ K}$ are absent. As for the observed variations in a temperature range of $110\text{--}120 \text{ K}$, they are referred either to the orientation transition glass–plastic crystal or to the polymorphic transformations in crystalline phases of ethanol (plastic crystal–monoclinic crystal transitions and $\alpha\text{--}\beta$ transformations in the monoclinic crystal) [12]. These processes and their detailed interpretation are out of the frameworks of this study.

3. CONCLUSIONS

Our investigations allow us to conclude that cryo-vacuum ethanol condensates formed at temperatures considerably lower than the glass transition (vitrification) temperature pass through the state, which can be characterized as the supercooled liquid phase, during the subsequent thermally stimulated transformations. The temperature range of the glass–liquid transformation is $97\text{--}100 \text{ K}$, which agrees well with the data of the authors who investigated the samples of solid ethanol obtained from the liquid phase. This conclusion can be confirmed by the following experimental results presented in this work.

(i) The variations in the IR spectrum of the sample, which was obtained upon heating to $T = 112 \text{ K}$ (Fig. 3), are observed. They manifest themselves in broadening of the absorption bands referred to the combinations of stretching vibrations $\nu(\text{CCO})$ with rotational vibrations of methyl $\nu(\text{CH}_3)$ and methylene $\nu(\text{CH}_2)$ groups and deformational vibrations of the $\delta(\text{OH})$ bond (the group of bands in a range of $1000\text{--}1250 \text{ cm}^{-1}$). In addition, these bands are noticeably shifted towards lower frequencies. The absorption band of stretching vibrations of the CCO bond is noticeably broadened and shifted into the red region; a fine structure in a form of spectral perturbations appears for this band. This is apparently associated with the fact that weaker intermolecular interaction and appearance of additional degrees of freedom are characteristic of the state of ethanol heated to $T = 112 \text{ K}$, for example, due to the unfrozen rotational subsystem of the supercooled liquid.

(ii) The analysis of thermograms presented in Figs. 4 and 5 indicates that starting from $T = 94 \text{ K}$, vitreous ethanol transforms into the supercooled liquid state. This process is accompanied by the clearly pronounced interference of laser radiation, which is the consequence of glass melting with the formation of the SCL and subsequent dissolution of a thin water film in it. This leads to an essential variation in the optical density of the medium. The results of similar observations for various angles of incidence of laser radiation can also confirm the assumption on the existence of a metastable liquid ethanol phase in this temperature range.

(iii) Investigations of the samples obtained at temperatures higher than the glass transition temperature do not reveal any features in the vicinity of the glass transition temperature, which indirectly confirms the above-formulated statements.

REFERENCES

1. P. W. Anderson, *Science* (Washington) **267**, 1615 (1995).
2. M. D. Ediger, C. A. Angell, and S. R. Nagel, *J. Phys. Chem.* **100**, 13 200 (1996).

3. P. G. Debenedetti, *J. Phys.: Condens. Matter* **15**, 1669 (2003).
4. I. Kohl, L. Bachmann, A. Hallbrucker, E. Mayer, and T. Loertingab, *Phys. Chem. Chem. Phys.* **7**, 3210 (2005).
5. G. P. Johar, *J. Chem. Phys.* **119**, 2935 (2003).
6. Y. Yue and C. Angell, *Nature (London)* **427**, 717 (2004).
7. A. Drobyshev, A. Aldiyarov, V. Kurnosov, and N. Tokmoldin, *Low Temp. Phys.* **33** (4), 355 (2007).
8. A. Drobyshev, K. Abdykalykov, A. Aldiyarov, V. Kurnosov, and N. Tokmoldin, *Low Temp. Phys.* **33** (8), 699 (2007).
9. O. Haida, H. Suga, and S. Seki, *J. Chem. Thermodyn.* **9**, 1133 (1977).
10. M. A. Ramos, S. Viera, F. J. Bermejo, J. Davidowski, H. E. Fischer, H. Schober, M. A. Gonzales, C. K. Loong, and D. L. Price, *Phys. Rev. Lett.* **78**, 82 (1997).
11. C. Talon, M. Ramos, S. Vieira, G. Guello, F. Bermejo, A. Griado, M. Senent, S. Bennington, H. Fischer, and H. Schober, *Phys. Rev. B: Condens. Matter* **58**, 745 (1998).
12. M. A. Ramos, I. Shmyt'ko, E. Arnautova, R. Jiménez-Riobóo, V. Rodríguez-Mora, S. Vieira, and M. J. Capitán, *J. Non-Cryst. Solids* **352**, 4769 (2006).
13. A. Aldiyarov, M. Aryutkina, A. Drobyshev, M. Kalkanov, and V. Kurnosov, *Low Temp. Phys.* **35** (4), 251 (2009).
14. A. Aldiyarov, M. Aryutkina, A. Drobyshev, and V. Kurnosov, *Low Temp. Phys.* **37** (6), 524 (2011).
15. A. Aldiyarov and A. Drobyshev, *Low Temp. Phys.* **37** (8), 718 (2011).
16. C. Talon, M. Ramos, and S. Vieira, *Phys. Rev. B: Condens. Matter* **66**, 012201-1 (2002).

Translated by N. Korovin

SPELL: OK